Computer Simulation of Heat and Mass Transfer in Permeable Media

MARCEL ROSCA[1], MIKLOS ANTICS[1], and KOSTAS KARYTSAS[2]
[1] Faculty of Energy Engineering
University of Oradea
1, Universitatii St., 410097 Oradea
ROMANIA
mrosca@uoradea.ro, m.antics@geoproduction.fr; http://www.uoradea.ro
[2] Geothermal Department
Centre for Renewable Energy Sources
19th km Marathonos Ave., 19009, Pikermi Attiki
GREECE
kkari@cres.gr; http://www.cres.gr

Abstract: - The University of Oradea had a research program on power generation from low enthalpy geothermal energy, before it became a partner in the LOW-BIN project, in which it is intended to build two demonstration units for power generation using geothermal water with about 85°C and slightly over 100°C. For this reason, it was considered interesting to built a numerical model of the well and surrounding rock to simulate the heat and mass transfer. The paper briefly presents the model setup, its calibration, and some simulation results.

Key-Words: - geothermal, modeling, simulation, TOUGH2.

1 Introduction

The City of Oradea, with a population of about 230,000, is located in the western part of Romania, some 10 km from the border with Hungary, on top of a low enthalpy geothermal reservoir. Between 1970 and 1980, 12 geothermal wells were drilled within the city limits. The depth of these wells range between 2,500 and 3,400 m, with well head temperatures of 70 to 105°C, and artesian flow rates of 5 to 35 l/s. All these wells are currently used, one for reinjection, and the others for production. One of the production wells is located on the University of Oradea campus.

The well from the University of Oradea campus is a typical low enthalpy geothermal well with multiple feed zones, about 3,000 m deep, 80÷85°C well head temperature, and about 30 l/s maximum artesian flow rate. As it was a potential location for one of the two demo units to be developed in the EC funded "Efficient Low Temperature Geothermal Binary Power" (acronym LOW-BIN), this well was used to study the heat transfer between the geothermal fluid and the surrounding rock during production at different flowrates. This was quite important, as it was intended to increase the produced flowrate form the maxim artesian 30 to 55 l/s by pumping.

The hydrodynamic and thermodynamic processes that occur during exploitation in the well and surrounding rock, from bottom to surface, are too complex for an exact analytical integration of the differential equations system.

A 3-D numerical model has been defined and used to simulate the heat transfer and the hydro-thermodynamic processes in the well and in the surrounding rock along the entire well. The paper presents the model's grid, the thermal and hydrodynamic properties of each block, the natural state simulation, as well as the static and dynamic calibrations.

After its calibration, the model was used to simulate the evolution of the pressure and temperature fields in the well and in the surrounding rock during artesian production at different flow rates.

2 The Oradea Geothermal Reservoir

Romania is located in Central Europe, North of the Balkan Peninsula, on the lower course of the Danube River, and on the Black Sea coast. The geological research carried out between 1960 and 1980 proved the existence of significant geothermal resources in some regions, mainly in the western part of the country. Over 200 drilled wells show the presence of geothermal resources, the proven reserves (by pumping the existing wells) being about 200,000 TJ for 20 years. The total installed capacity of the existing wells for energy uses is 320 MW_t (for a 30°C reference temperature). The main uses of geothermal energy in Romania are: space and tap water heating, greenhouse heating, health and recreational bathing, industrial process heat, and fish farming [11].

The Oradea geothermal reservoir comprises two specific aquifers that are hydraulically connected, namely: the Triassic aquifer Oradea and the Cretaceous aquifer Felix Spa.

The Felix Spa reservoir is currently exploited by 6 wells, 50 to 450 m deep. The total artesian flow rate available from these wells is 210 l/s. The water is produced at a wellhead temperature of 36 to 48°C and is only used for recreational and health bathing.

The Oradea aquifer is located in Triassic limestone and dolomites, at depths of 2,200 to 3,400 m. The reservoir covers an area of about 113 km^2, and is exploited by 12 wells, with a total artesian flow rate of 140 l/s and well head temperatures of 70 to 105°C. The water is of calcium-sulphate-bicarbonate type, with no scaling or corrosion potential. There are no dissolved gases, and the TDS is lower than 0.9 to 1.2 g/l. The total installed capacity is over 30 MW_t.

The reservoir is bounded by faults. There are also internal faults in the reservoir, dividing it into four hydraulically connected blocks. The source of the geothermal fluid is located in the north-eastern part of the reservoir, along preferential pathways represented by the fault system at the boundary. A cross section through the reservoir is shown in Figure 1.

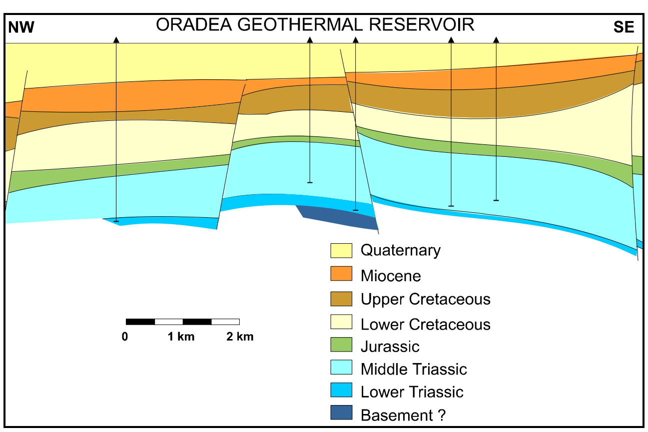

Fig. 1: Cross section through the Oradea reservoir

The terrestrial heat flow is about 90 mW/m^2, and the geothermal gradient 2.6-4.1°C/100 m. Properties such as ionic composition, high radioactivity and the content of rare gases, indicate an active circulation along paths partially in contact with the crystalline basement.

The natural recharge rate was calculated at about 300 l/s based on the only interference test by now, carried out in 1979 [4]. The hydro-geological [2], hydro-chemical [12], and geothermal [13] research proved that the reservoir is recharged via a deep pathway along an important structural line (the Velenta fault, oriented NE-SW), excluding the lateral recharge. The water in the Oradea aquifer is about 20,000 years old.

The convective system in the Oradea area is recharged from the East, mainly through the system of faults and fractures delineating the Borod basin (about 20-30 km east of Oradea), but also through strata surfaces. Cold waters infiltrated in the karstic areas of the Padurea Craiului Mountains are flowing westward and downward, reaching higher temperature layers, and are starting the thermal convection process in the entire Triassic carbonate stack, 500 to 800 m thick.

During the 1980's, most (usually all 12) wells used to be logged almost every year, usually once in spring, after the end of the heating season, and once in fall, before the start of the new heating season. The only logging campaign since the 1989 has been carried out in 1995, in order to collect new and more reliable data for a 2D reservoir model. Based on all available data (geology, hydrology, well tests and logs, and production history) as well as on the reservoir simulation [1], the following mean values have been determined for the rock matrix:

- density: $\rho_r = 2,750$ kg/m^3;
- effective porosity: $\Phi = 1.8$-2.0%;
- permeability: $k_r = 230$ mD;
- specific heat capacity: $c_r = 1,030$ J/kg·K;
- thermal conductivity:
  $\lambda_r = 3.72$ W/m·K for Triassic dolomite;
  $\lambda_r = 3.00$ W/m·K for Triassic limestone;
  $\lambda_r = 2.79$ W/m·K for Lower Cretaceous limestone;
  $\lambda_r = 3.20$ W/m·K for Upper Cretaceous limestone;
- transmissivity: T = 211 D·m.

3 The Geothermal Well Completion

The geothermal well from the University of Oradea campus was completed in 1981 and initially produced in artesian discharge 2.5 l/s geothermal fluid with a wellhead temperature of 68°C. After the acid job carried out in 1983 (1,500 m^3 of 1.5% HCl solution), the artesian flow rate increased to 31 l/s, and the well head temperature reached 85°C. The well is producing, at different flow rates, almost continuously since the acid job of 1983. The geothermal water is used to supply space heating and hot tap water to the campus and some blocks of flats in the vicinity.

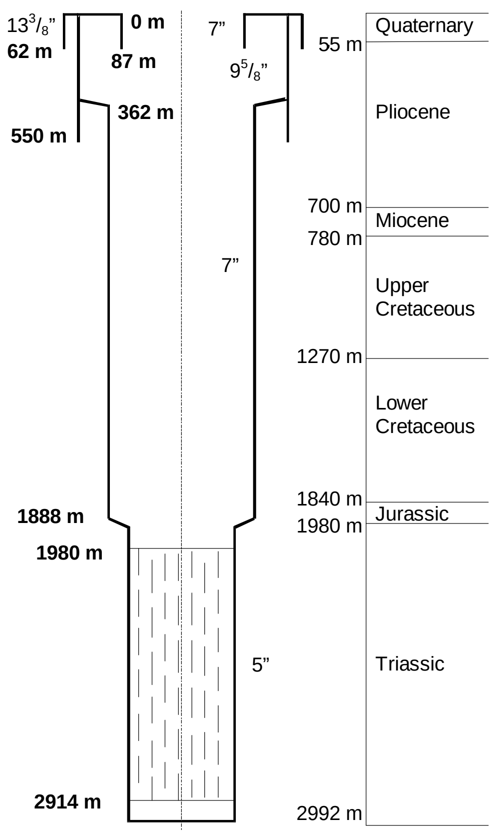

Fig. 2: Well completion and geological strata

The well (as most of the wells in Romania) was usually logged twice per year, in spring and in fall. All pressure and temperature logs between 1981 and 1995 were compared and analyzed, the most reliable being considered the latest, of July 30th, 1995, this being the only time when electronic gauges were used to log the well, both in static and dynamic conditions. Mechanical gauges, with a much lower precision, have been used for all previous logs, and no more logging campaign was carried out after 1995 (it was considered too expensive, the continuous monitoring of the production parameters being considered sufficient).

Figure 2 shows the completion of the geothermal well and the geological strata identified during drilling. The casings ($13^{3}/_{8}$", $9^{5}/_{8}$", and 7") are cemented.

The hydro-thermodynamic properties of the rocks from all geological strata penetrated by the well, form the University of Oradea campus, as well as the layers thickness, as determined during drilling, in Table 1.

Table 1: Geological strata and rock properties

Layer	Δh [m]	ρ [kg/m³]	λ [W/m·K]	c [J/kg·K]	a [m²/s]
1	60	1.800	0,97	867	$6{,}216 \cdot 10^{-07}$
2	302	1.950	2,89	873	$1{,}698 \cdot 10^{-06}$
3	188	2.000	2,17	885	$1{,}226 \cdot 10^{-06}$
4	150	2.000	2,11	885	$1{,}192 \cdot 10^{-06}$
5	80	2.100	2,25	900	$1{,}190 \cdot 10^{-06}$
6	490	2.200	3,50	925	$1{,}720 \cdot 10^{-06}$
7	570	2.300	3,95	967	$1{,}776 \cdot 10^{-06}$
8	140	2.500	9,00	988	$3{,}644 \cdot 10^{-06}$
9	1.010	2.750	2,43	1.030	$8{,}579 \cdot 10^{-07}$

The layers numbered in Table 1, place below each other, represent geological strata, which are:

1. Quaternary
2. Upper Pliocene
3. Lower Pliocene 1
4. Lower Pliocene 2
5. Miocene
6. Upper Cretaceous
7. Lower Cretaceous
8. Jurassic
9. Triassic

The thermal conductivity of the rocks in each layer has been calculated with the steady state heat conduction equation, knowing that the terrestrial heat flow density is 90 mW/m^2, and using the temperature log of September 23rd, 1984, when the well was shut in for 10 days. It has been assumed that the shut in time was long enough to reach the thermal equilibrium, so that the water had the same temperature as the rock in natural state at the same depth. The truth level of this assumption could not be determined with the available measured data.

4 The Numerical Model

The PC version of the TOUGH2 computer code was used to model the geothermal well.

A cylindrical model was defined, with the external radius of 10 km, for the outermost elements certainly not to be affected by the heat exchange with the geothermal fluid flowing in the well, and also for the modeled reservoir to be about the same size as the real one (in surface and thickness), although not the same shape.

For the natural state simulation, the model was divided into 36 cylindrical blocks on top of each other. The thickness of each block was selected so that the block could be considered homogeneous and the center of most of them to correspond to usual stations of well logs.

Two more blocks were added, one on top and the other below. The top block was defined to simulate the atmosphere, with zero volume for constant pressure and temperature conditions (for the Oradea area, annual mean values of 1 bar and 10.2°C). The bottom block was defined as very thin, with thermal and hydraulic properties of an impermeable rock, to supply the natural heat flow of 90 mW/m^2.

Each of the 36 rock blocks was then divided into 28 coaxial cylindrical blocks. The radial increment was smaller for the first 18 blocks and selected such as to correspond to the well completion (casings, cement, and borehole), and after that in geometrical progression up to 100 m. The outside radius of the 19th block was 1,000 m, and for the outer 9 blocks the radial increment was 1,000 m.

To simulate the well head, one block was defined on top of the well, with hole properties, and connected on the lower side to the 3 coaxial blocks inside the $9^5/_8$" casing. This block is separated from the atmosphere by a steel block connected at the lower part to the upper part of the $9^5/_8$" casing.

5 Model Calibration

The calibration of the numerical model has been carried out by an iterative process, through the following steps:

1) model the natural state of the rocks (before the well was drilled);
2) model the stabilized static regime of the well;
3) simulate the production history;
4) compare calculated with measured data;
5) modify the values of some parameters and start over.

The initial conditions for the natural state simulation were selected equal to the local annual mean atmospheric conditions (1 bar and 10.2°C), constant with depth. The thermal regime stabilized after about 1.2 million years, which is practically the approximate time of the geological evolution of the reservoir.

The temperature gradient varies with depth, due to different thermal conductivities of different rocks. The variation of pressure with depth is also not linear, as it largely depends on the rock temperature and porosity, even for rocks with relatively high permeability. Fig. 3 shows the simulated temperature and pressure fields in the natural state.

The pressure and temperature fields in the natural state have been used as initial condition for the next stage, the simulation of the stabilized static regime of the geothermal well, when it has been closed for a long time and is in thermal equilibrium with the surrounding rock.

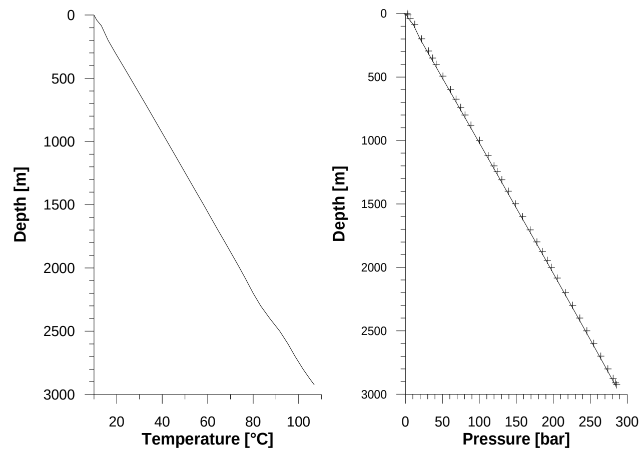

Fig. 3: Temperature and pressure fields in the natural state

The simulated thermal equilibrium is reached after about 3 hours. This time has no real meaning, as the simulation did not consider the pressure, and mainly the temperature, fields perturbation during drilling. Stabilized static regime simulation is needed to define the initial conditions in each block.

In stabilized static regime, the simulated difference between the temperature of the fluid inside the well and the rock temperature at the same depth (in the natural state) does not exceed 0.1°C. As regarding the pressure, the difference is more significant. In Figure 3, the continuous curve represents the natural state pressure field.

The production history, starting after the acid job in 1981 until August 30th, 1995, the date of the well logs used for both static and dynamic regime calibrations, is shown in Figure 4.

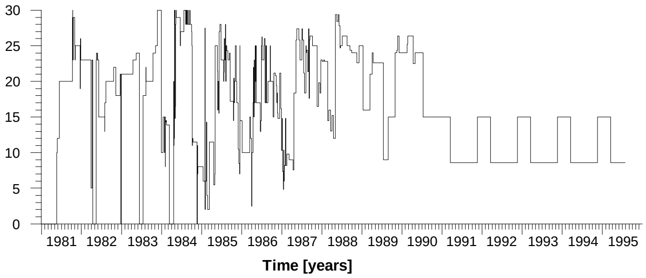

Fig. 4: Production history

The well logs of August 1995 have been used for both dynamic and static calibrations of the model, these being the only ones for which electronic gages were used, therefore having a reliable accuracy. The well produced 14.5 l/s during logging in dynamic condition. The well was then shut down for 6 hours. To compare the calculated pressure and temperature values in the well with the measured ones, for the dynamic calibration a 14.5 l/s production was simulated for 24 hours. Then, for the static calibration, the shut down well was simulated for the next 6 hours. The dynamic calibration is shown in Figure 5, and the static one in Figure 6.

For the dynamic calibration, significant errors occur at the upper part of the well, mainly due to the fact that at the logging date (August 1995) the well had a $5^1/_2$" tubing down to 200 m. This was not included in the model, as TOUGH2 does not calculate the heat exchange by radiation, and the production tubing was to be removed when the line shaft pump is installed in the well.

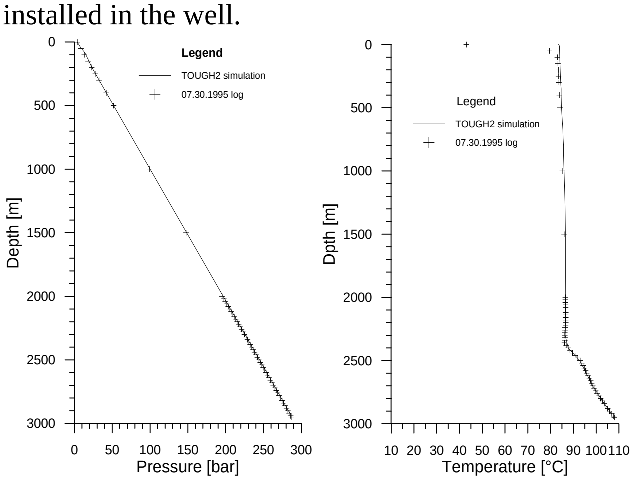

Fig. 5: Dynamic pressure and temperature calibration

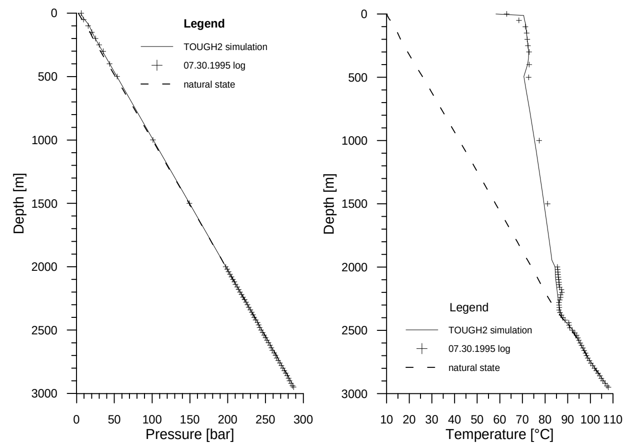

Fig. 6: Static pressure and temperature calibration

The correlation between the calculated and measured data is very good for the lower part of the well, along the reservoir, where measurement points are closer to each other. It was, therefore, possible to have a more accurate selection of the thermal and hydraulic parameters of the rock matrix in the vicinity of the modeled well.

Table 2: Hydro-thermal properties of materials

Layer		ρ	Φ	k	λ	c
no	type	kg/m^3	-	m^2	W/m·K	J/kg·K
1	Quat. (1)	1,800	0.30	1.00E-12	2.667	871.6
2	Quat. (2)	1,900	0.30	1.00E-12	2.989	885.6
3	U. Pl.	1,950	0.25	5.00E-13	2.821	892.7
4	L. Plio. (1)	2,000	0.20	5.00E-13	2.621	906.1
5	L. Plio. (2)	2,000	0.20	5.00E-13	2.751	911.3
6	Mio.	2,100	0.10	1.00E-13	2.761	914.2
7	U. Cret.	2,200	0.15	2.00E-13	2.777	917.6
8	L. Cret.	2,300	0.10	2.00E-13	2.789	919.7
9	Jurassic	2,500	0.05	1.00E-20	2.871	923.3
10	Tria. (1)	2,750	0.10	1.00E-20	3.212	1,030.0
11	Tria. (2)	2,750	0.10	6.00E-13	2.253	1,030.0
12	Tria. (3)	2,750	0.10	5.00E-20	2.277	1,030.0
13	Tria. (4)	2,750	0.10	4.00E-15	2.797	1,030.0
14	Tria.(5)	2,750	0.10	1.60E-12	1.827	1,030.0
15	Tria. (6)	2,750	0.10	4.00E-14	3.112	1,030.0
16	Tria. (7)	2,750	0.10	7.50E-14	2.277	1,030.0
17	Tria. (8)	2,750	0.10	2.30E-14	2.797	1,030.0
18	Tria. (9)	2,750	0.10	8.00E-14	3.112	1,030.0
19	Bottom	2,750	0.10	0	2.277	1,030.0
20	Air	1.12	0.9999	5.00E-11	0	1,000.0
21	Well hole	1,000	0.9999	1.80E-06	0.800	4,200.0
22	Steel	7,850	0.00	0	54.000	477.0
23	Cement	2,250	0.01	1.00E-20	2.836	760.0

Table 2 gives the thermal and hydraulic properties of all the materials defined for the blocks, as resulted after the static and dynamic calibrations. Densities and heat capacities of rocks and cement have been calculated as functions of temperature [7], as well as the thermodynamic properties of the geothermal fluid [8].

As also indicated by some data available from drilling, the Triassic rocks are not all calcite and dolomites, being mixed with clays and marls, so that the Triassic layers have different properties. The strata above the reservoir are homogeneous.

The values determined during the calibration are different from those given in Table 1 mainly in the upper layers (younger and less consolidated), mainly due to water content.

6 Production Simulation Results

After the static and dynamic calibration, it is possible to simulate any desired production or injection scenario and to obtain the evolution in time of the pressure and temperature fields in the well and in the surrounding rocks. The fluid flow rate and heat flux transferred between each pair of blocks of the defined model can also be simulated. It is then possible to find the influence of the mass or volume flow rate on wellhead pressure, wellhead temperature, total heat flux lost in the well, specific heat loss, specific enthalpy drop, etc.

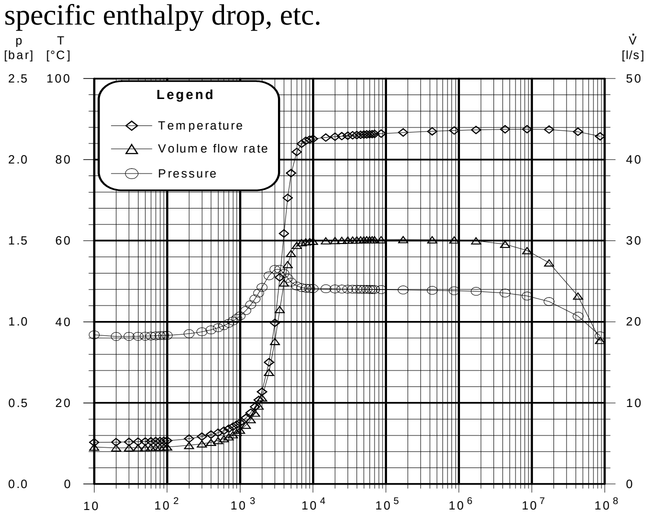

Fig. 7: Simulated flow rate, well head pressure, and well head temperature for full artesian flow

After the model's calibration, artesian production at full flow rate (30 l/s) has been simulated for 10^8 s (about 3 years). The simulated parameters are shown in Figure 7.

The simulation showed three distinct stages of the well's evolution in time.

During the first stage, which lasts $6{\cdot}10^3$ to $7{\cdot}10^3$ seconds (about 2 hours), the cold fluid is removed from the well, being replaced by the hot fluid flowing in from the reservoir. In the first few seconds after the well head valve is fully opened, due to the incompressibility of water, the well head pressure falls from 2.28 bar (the value in stabilized static regime) to 0.8 bar. Thus, the well can only be started by gradually opening the valve, which corresponds to the real situation. As the hot fluid is replacing the cold one in the well, the hydrostatic pressure decreases, therefore the well head pressure increases, reaching a maximum after about $2{\cdot}10^3$ seconds. Then, the well head pressure decreases slightly, as the pressure drop in the rock around the well increases due to the rapid increase of the flow rate. During this stage, when the wellbore storage effect is dominant, both the hydraulic and thermal regimes are highly transitory, the pressure and temperature fields varying fast, mainly in the blocks defined inside and close around the well.

The thermal and hydraulic regimes in the second stage are also transitory, but the temperature and pressure variations are much slower, both in the well and surrounding rock. The well head temperature increases with less than 2°C during 200 days of full flow production. The artesian flow rate continues to slowly increase, due to hydrostatic pressure decrease, then starts to decrease, as well as the well head pressure, due to the reservoir pressure decrease.

The temperature and pressure profiles in the well, and the heat flux lost to the surrounding rock, do not vary significantly during this stage, as well as the total heat flux lost in the well (Figure 8), because the casing, the cement, and the rocks close to the well are already heated, and as the heat exchange area increases with the square of the radius, so that the heat flux density (W/m^2) tends to become negligible at a few tens of meters from the well. Therefore, both the thermal and hydraulic regimes in the well may be considered as *quasi-steady* during this second stage.

The *quasi-steady* regime is also confirmed by the variation in time of the linear density of the heat flux [W/m] lost in the well above the geothermal reservoir (Figure 9).

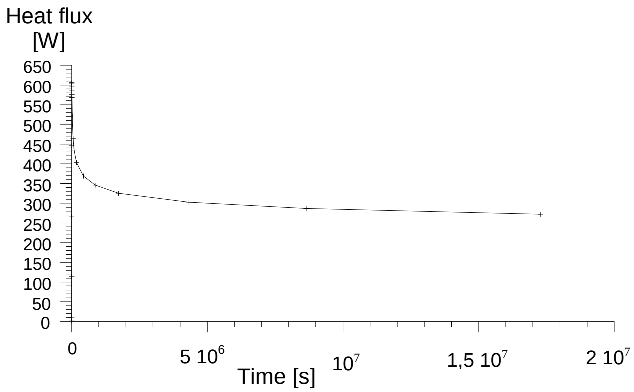

Fig. 8: Total heat flux lost in the well above the reservoir for the maximum artesian flow rate (30 l/s)

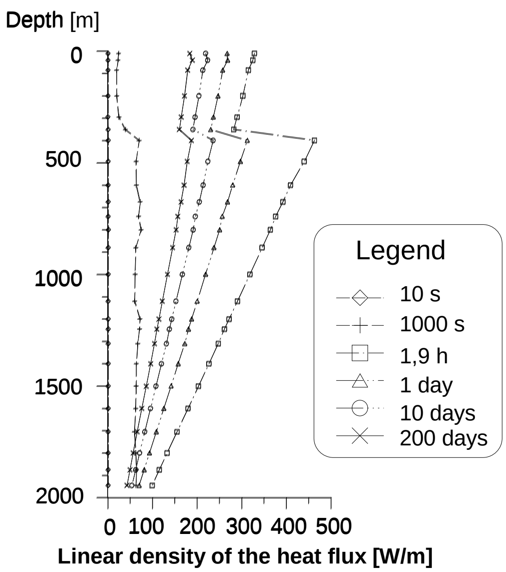

Fig. 9: Linear density of the heat flux above the aquifer

Based on the numerical simulation results, it was possible to calculate that during the *quasi-steady* state the coefficient of convection in the well vary by less than 1% with depth and time, being only function of the fluid velocity. For the full artesian flow, it was about 18 $W/m^2 \cdot K$ in the $9^5/_8$" casing, and 6.5 $W/m^2 \cdot K$ in the 7" casing. Furthermore, it was possible to verify the assumption proposed by Ramey [5] and adopted by Ortiz-Ramirez [3] that the thermal resistance of the convection in the well is negligible compared to the thermal resistance of the conduction in a infinite radius cylindrical wall. This assumption is obviously true for an infinite radius cylindrical wall, but the numerical simulation shows that, at least for a low temperature well, the temperature field in the rock at 100 m from the well is not perturbed after up to 30 years of full flow production. In these conditions, the thermal resistance of the convection is not negligible, being 20 to 25% of the thermal resistance of conduction in the 100 m thick cylindrical wall.

The third stage shows, in Figure 6, after about $2 \cdot 10^6$ s. The artesian flow rate and the well head pressure are both decreasing relatively fast, due to the depletion of the modeled reservoir, which is closed, unlike the real one. As the main target was to model the well, and not the reservoir, this stage has no real meaning. It only confirms once again that the simulator works correctly. It may also be used to calibrate a full model of the reservoir, including all wells and its border conditions, such as natural recharge.

The calculated wellhead temperature for different flow rates in the *quasi-steady* regime is shown in Figure 10.

Because the wellhead temperature slowly increases, even during the *quasi-steady* regime, production was simulated for 2 to 10 days (or longer for smaller flow rates), thus reaching the *quasi-steady* regime and also avoiding the occurrence of a significant pressure drop in the modeled reservoir.

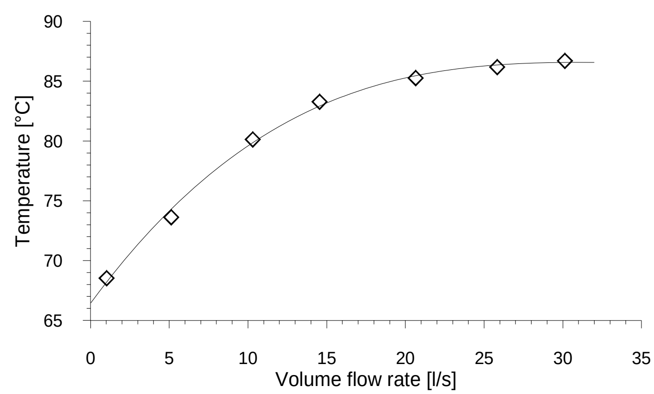

Fig. 10: Well head temperature variation with flow rate

Based on the simulated values, it was possible to find the following equation of the wellhead temperature as a function of the production volume flow rate:

$$T_{WH} = 66.444 + 1.791\,\dot{V} - 5.278 \cdot 10^{-2}\,\dot{V}^2 + 5.144 \cdot 10^{-4}\,\dot{V}^3. \quad (1)$$

where: T_{WH} [°C] - well head temperature;
$\dot{V}$ [l/s] - production volume flow rate.

Equation 1 may confidently be used to estimate the well head temperature of the modeled well even for production flow rates at least 50% higher than the maximum artesian one, which would represent the installation of a deep well pump to increase production. For a more accurate estimate, a new model has to be set up, which should include the model of the specific pump to be installed in the well.

The simulation results have also been used to obtain the deliverability curve (Figure 11) for the modeled well (wellhead pressure as a function of the production flow rate), as well as the deliverability Equation 2, using the same methodology as for Figure 10 and Equation 1. These may be used to estimate the depth at which a certain pump should be set in the well.

$$p_{WH} = 4.08 + 9.35 \cdot 10^{-2}\dot{V} - 1.97 \cdot 10^{-2}\dot{V}^2 + 6.42 \cdot 10^{-4}\dot{V}^3 - 7.755 \cdot 10^{-6}\dot{V}. \quad (2)$$

where: p_{WH} [bar] - well head temperature;
$\dot{V}$ [l/s] - production volume flow rate.

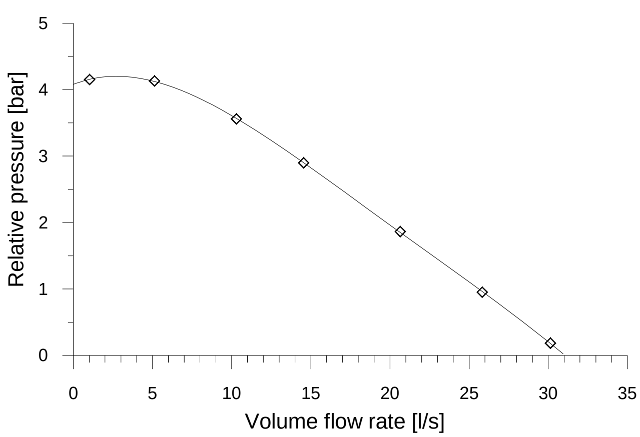

Fig. 11: Calculated deliverability curve

For the *quasi-steady* regime, Figure 12 shows the total heat flux lost in the well and the specific heat loss per unit mass (calculated as the ratio between the heat flux and the mass flow rate) as functions of mass flow rate. At small flow rates, the specific heat loss and therefore the specific enthalpy decrease along the well is more significant, resulting in a more severe temperature decrease, a lower average temperature in the well, and thus a lower value for the total heat flux lost in the well.

As the flow rate increases, the fluid velocity in the well and the convection coefficient also increase, therefore the total lost heat flux increases, whereas the specific heat loss and the specific enthalpy drop decrease, resulting in a lessening of the temperature drop in the well, therefore a higher average temperature in the well and a higher wellhead temperature.

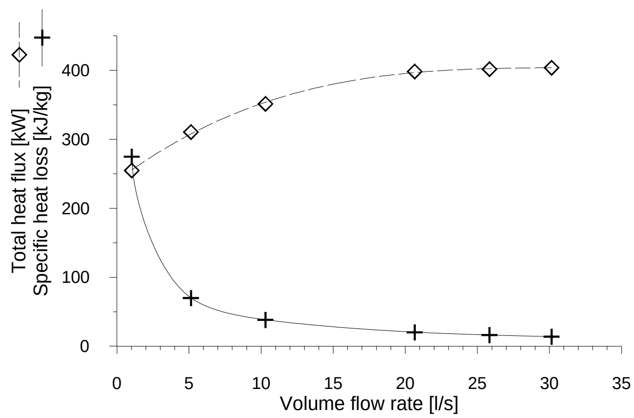

Fig. 12: Heat loss as a function of flow rate

In low enthalpy wells, in which boiling cannot occur, it is possible that there would only be a small specific enthalpy drop along the well (due to the specific heat loss) at high flow rates. Therefore, as the hydrostatic pressure decreases with depth, the fluid temperature does not decrease, but slightly increase. For the modeled well, at a flow rate of 30 l/s, the temperature in the cased part of the well (above the reservoir) increases by about 1°C before decreasing again close to the wellhead.

7 Influence on the Surrounding Rocks

The simulator calculates the pressure and temperature values in the centre of each block defined in the model at the time steps set in the input file.

Production at the maximum artesian discharge flow rate (30 l/s) was simulated for a long period of time in order to study its influence on the temperature (and pressure) field in the rocks around the well. The influence becomes more important with the decrease of the depth, as the natural state temperature increases with depth. Figures 13 and 14 depict the variation in time of the temperature field in two relevant layers, one with the centre at the depth of 10 m (where the well is cased with the $9^5/_8$" casing), and the other one with the centre at the depth of 400 m (where the well is cased with the 7" casing).

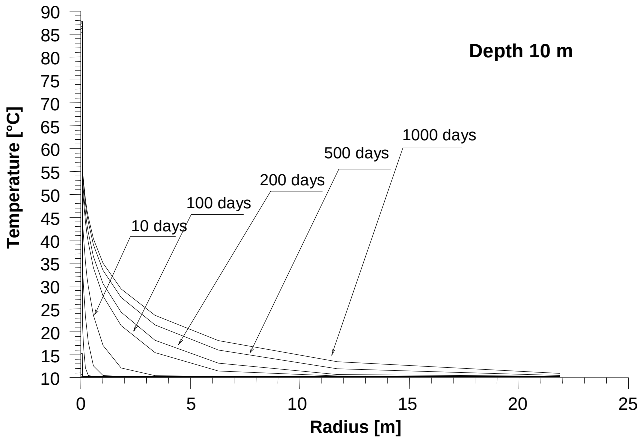

Fig. 13: Temperature field during production, at the depths of 10 m

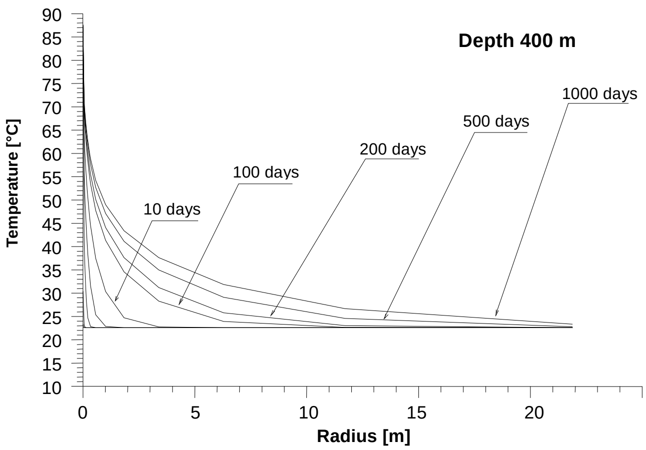

Fig. 14: Temperature field during production, at the depths of 400 m

The temperature increases very fast just close to the well, but the influence of the heat lost from the geothermal fluid flowing in the well is negligible at about 25 m radius even after 3 years of continuous production. Of course, the area of the isothermal surfaces increases with the second power of the radius, as well as the volume of the rock blocks which accumulate heat and in which the temperature increases as a linear function of the accumulated heat. This does not mean that the thermal regime is stationary. It is still transient, but at a very low rate.

To study the return of the temperature field around the well back to the natural state after a long time production, the model was used to simulate the production at the maximum artesian discharge flow rate for 172 days (the average heating season in the Oradea area), and then the well was shut down. The heat accumulated in the rock around the well is dissipated by conduction, which is expected to be a rather slow process, the thermal conductivity of the rocks being relatively low, even in porous rocks saturated with water. Figures 15 and 16 depict the variation in time of the temperature field around the well in the same two layers as in Figures 13 and 14.

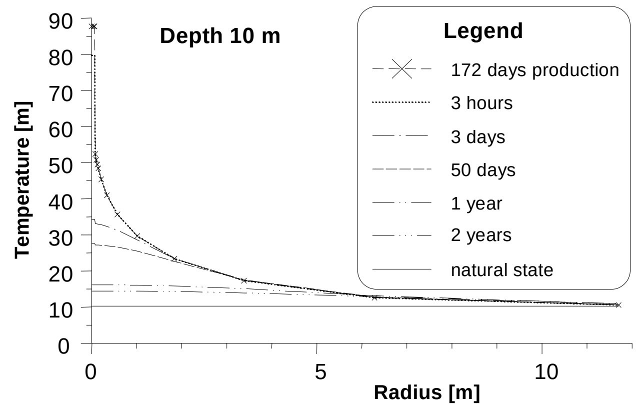

Fig. 16: Temperature field with the shut down well, at the depths of 10 m

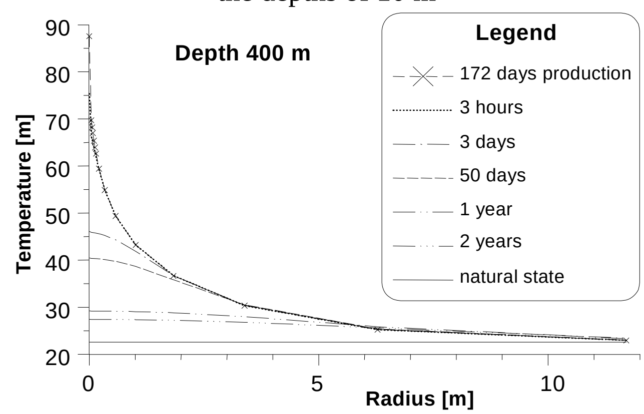

Fig. 15: Temperature field with the shut down well, at the depths of 400 m

In a few days after the well is shut down, the temperature of the fluid inside the well reaches the casing temperature, but higher than the natural state temperature of the respective layer. The rock temperature close to the well decreases slowly, by dissipating the heat to the neighbouring layers, the temperature at a higher distance increasing slightly. The temperature in the well and surrounding rock will eventually reach the natural state value, but only after a very long time (at least 15÷20 years) of keeping the well shut after production for a significant time (one heating season) and at a significant flow rate (30 l/s during simulation).

8 Conclusion

A calibration based on accurate measured data provides good estimates of the thermodynamic and hydrodynamic properties of all materials, including casings and cement, being even possible to identify some problems, such as scaling and corrosion in the well (from pressure losses), or cracks in the cement (from heat losses).

After the calibration, it is possible to simulate any desired production or injection scenario and to obtain the evolution in time of the pressure and temperature fields in the well and in the surrounding rocks. The fluid flow rate and heat flux transferred between each pair of blocks of the defined model can also be simulated. It is then possible to find the influence of the mass or volume flow rate on wellhead pressure, wellhead temperature, total heat flux lost in the well, specific heat loss, specific enthalpy drop, etc.

It was also possible to verify the assumption proposed by Ramey [5], and adopted by Ortiz-Ramirez [3], that the thermal resistance of convection in the well is negligible as compared to the thermal resistance of conduction in a cylindrical wall of infinite radius. The assumption is obviously true for an infinite radius cylindrical wall, but the numerical simulation shows, at least for a low temperature system, that the temperature field in the rock at 100 m from the well is not perturbed after 30 years of full flow production. In these conditions, the thermal resistance of convection is not negligible, being about 20-25% of the thermal resistance of conduction in a 100 m thick cylindrical wall.

References:

[1] Antics, M. A. (1996): Computer Simulation of Oradea Geothermal Reservoir. In: *Proceedings of the 22nd Geothermal Reservoir Engineering Workshop*, Stanford, CA, pp. 491-496.

[2] Cohut, I., Paál, G. (1985): Study on the Hydro-dynamic Connection between the Oradea and Felix Geothermal Areas, I.F.L.G.S. archive, Bucharest (in Romanian).

[3] Ortiz-Ramirez, J. (1983): *Two-phase Flow in Geothermal Wells, Development and Uses of a Computer Code*. Stanford Geothermal Program Report SGP-TR-66, Stanford University, Stanford, CA., USA.

[4] Paál, G. (1979): Calculation of the Underground Thermal Water Resource from the Cretaceous Felix Spa Reservoir, I.I.S. archive, Oradea (in Romanian).

[5] Ramey, H. J. (1962): Wellbore Heat Transmission. In: *Journal of Petroleum Technology*, **225**, 427-435.

[6] Rosca, M. (1997 a), "Thermodynamic Properties of Geothermal Wells", Proceedings of the University of Oradea Annual Symposium, Energy Engineering volume, Oradea, Romania, 144-149, (*in Romanian*).

[7] Rosca, M. (1997 b), "Hydraulic and Thermal Properties of Rocks Common in Geothermal Areas", Proceedings of the University of Oradea Annual Symposium, Energy engineering volume, Oradea, Romania, 150-155, (*in Romanian*).

[8] Rosca, M., and Antics, M. (1997), "Hydraulic and Thermal Properties of Geothermal Fluids", Proceedings of the University of Oradea Annual Symposium, Energy engineering volume, Oradea, Romania, 156-161, (*in Romanian*).

[9] Rosca, M. (1998): *Contributions to the modelling of heat transfer in geothermal wells*. Ph.D. Thesis, University of Oradea, Romania, 169 pp. (*in Romanian*).

[10] Rosca, M., and Antics, M. (1999): Numerical Model of the Geothermal Well Located at the University of Oradea Campus. *Proceedings of the 24th Geothermal Reservoir Engineering Workshop*, SGP-TR-162, Stanford, CA.

[11] Rosca, M., Antics, M., Sferle, M. (2005): *Geothermal Energy in Romania: Country Update 2000-2004*, Proceedings of the World Geothermal Congress 2005, Antalya, Turkey.

[12] Tenu, V. et al. (1979): Isotopic Research on the Geothermal Waters Romanian Western Plain, I.I.R.G., Pisa, Italy.

[13] Veliciu, S., Zamfir, A. (1986): Geothermal Study of the Oradea – Felix Spa Area, Theme A 9.a., Romanian Geological Survey archive, Bucharest, (in Romanian).